BELLE Preprint 2014-8
KEK Preprint 2014-2

arXiv:1406.6356v4 [hep-ex] 25 Mar 2015

# Search for $B^+ \to e^+\nu$ and $B^+ \to \mu^+\nu$ decays using hadronic tagging

## Abstract

We present a search for the rare leptonic decays $B^+ \to e^+\nu_e$ and $B^+ \to \mu^+\nu_\mu$, using the full $\Upsilon(4S)$ data sample of $772 \times 10^6$ $B\bar{B}$ pairs collected with the Belle detector at the KEKB asymmetric-energy $e^+e^-$ collider. One of the $B$ mesons from the $\Upsilon(4S) \to B\bar{B}$ decay is fully reconstructed in a hadronic mode, while the recoiling side is analyzed for the signal decay. We find no evidence of a signal in any of the decay modes. Upper limits of the corresponding branching fractions are determined as $\mathcal{B}(B^+ \to e^+\nu_e) < 3.5 \times 10^{-6}$ and $\mathcal{B}(B^+ \to \mu^+\nu_\mu) < 2.7 \times 10^{-6}$ at 90% confidence level.

PACS numbers: 13.20.-v, 13.25.Hw, 12.15.Hh

Y. Yook,[70] Y.-J. Kwon,[70] A. Abdesselam,[58] I. Adachi,[12] S. Al Said,[58,27] K. Arinstein,[4] D. M. Asner,[49] V. Aulchenko,[4] T. Aushev,[22] R. Ayad,[58] S. Bahinipati,[15] A. M. Bakich,[57] A. Bala,[50] V. Bansal,[49] V. Bhardwaj,[41] B. Bhuyan,[16] A. Bondar,[4] G. Bonvicini,[68] A. Bozek,[45] M. Bračko,[34,23] T. E. Browder,[11] D. Červenkov,[5] V. Chekelian,[35] A. Chen,[42] B. G. Cheon,[10] K. Chilikin,[22] R. Chistov,[22] K. Cho,[28] V. Chobanova,[35] Y. Choi,[56] Z. Doležal,[5] Z. Drásal,[5] A. Drutskoy,[22,37] D. Dutta,[16] K. Dutta,[16] S. Eidelman,[4] H. Farhat,[68] J. E. Fast,[49] T. Ferber,[7] O. Frost,[7] V. Gaur,[59] N. Gabyshev,[4] S. Ganguly,[68] A. Garmash,[4] R. Gillard,[68] R. Glattauer,[19] Y. M. Goh,[10] B. Golob,[32,23] O. Grzymkowska,[45] J. Haba,[12] K. Hara,[12] K. Hayasaka,[40] H. Hayashii,[41] X. H. He,[51] M. Heck,[25] T. Higuchi,[26] Y. Horii,[40] Y. Hoshi,[62] W.-S. Hou,[44] T. Iijima,[40,39] A. Ishikawa,[63] R. Itoh,[12] Y. Iwasaki,[12] T. Iwashita,[26] I. Jaegle,[11] T. Julius,[36] E. Kato,[63] P. Katrenko,[22] T. Kawasaki,[47] C. Kiesling,[35] D. Y. Kim,[55] J. B. Kim,[29] J. H. Kim,[28] K. T. Kim,[29] M. J. Kim,[30] Y. J. Kim,[28] K. Kinoshita,[6] J. Klucar,[23] B. R. Ko,[29] P. Kodyš,[5] S. Korpar,[34,23] P. Križan,[32,23] P. Krokovny,[4] T. Kuhr,[25] A. Kuzmin,[4] J. S. Lange,[8] Y. Li,[67] L. Li Gioi,[35] C. Liu,[53] Y. Liu,[6] D. Liventsev,[12] P. Lukin,[4] K. Miyabayashi,[41] H. Miyata,[47] G. B. Mohanty,[59] A. Moll,[35,60] R. Mussa,[21] Y. Nagasaka,[13] I. Nakamura,[12] E. Nakano,[48] M. Nakao,[12] Z. Natkaniec,[45] M. Nayak,[17] E. Nedelkovska,[35] N. K. Nisar,[59] S. Nishida,[12] O. Nitoh,[66] S. Ogawa,[61] S. Okuno,[24] P. Pakhlov,[22,37] C.-S. Park,[70] H. Park,[30] H. K. Park,[30] T. K. Pedlar,[33] R. Pestotnik,[23] M. Petrič,[23] L. E. Piilonen,[67] M. Ritter,[35] M. Röhrken,[25] A. Rostomyan,[7] S. Ryu,[54] T. Saito,[63] Y. Sakai,[12] S. Sandilya,[59] L. Santelj,[23] T. Sanuki,[63] Y. Sato,[63] V. Savinov,[52] O. Schneider,[31] G. Schnell,[1,14] C. Schwanda,[19] K. Senyo,[69] O. Seon,[39] M. E. Sevior,[36] V. Shebalin,[4] C. P. Shen,[2] T.-A. Shibata,[64]

J.-G. Shiu,[44] B. Shwartz,[4] A. Sibidanov,[57] F. Simon,[35,60] Y.-S. Sohn,[70] A. Sokolov,[20] E. Solovieva,[22] M. Starič,[23] M. Steder,[7] M. Sumihama,[9] T. Sumiyoshi,[65] G. Tatishvili,[49] Y. Teramoto,[48] K. Trabelsi,[12] M. Uchida,[64] T. Uglov,[22,38] P. Urquijo,[3] Y. Usov,[4] C. Van Hulse,[1] P. Vanhoefer,[35] G. Varner,[11] K. E. Varvell,[57] A. Vinokurova,[4] V. Vorobyev,[4] M. N. Wagner,[8] C. H. Wang,[43] M.-Z. Wang,[44] P. Wang,[18] X. L. Wang,[67] M. Watanabe,[47] Y. Watanabe,[24] S. Wehle,[7] K. M. Williams,[67] E. Won,[29] Y. Yamashita,[46] S. Yashchenko,[7] Y. Yusa,[47] Z. P. Zhang,[53] V. Zhilich,[4] and A. Zupanc[23]

(The Belle Collaboration)

[1]*University of the Basque Country UPV/EHU, 48080 Bilbao*

[2]*Beihang University, Beijing 100191*

[3]*University of Bonn, 53115 Bonn*

[4]*Budker Institute of Nuclear Physics SB RAS and Novosibirsk State University, Novosibirsk 630090*

[5]*Faculty of Mathematics and Physics, Charles University, 121 16 Prague*

[6]*University of Cincinnati, Cincinnati, Ohio 45221*

[7]*Deutsches Elektronen–Synchrotron, 22607 Hamburg*

[8]*Justus-Liebig-Universität Gießen, 35392 Gießen*

[9]*Gifu University, Gifu 501-1193*

[10]*Hanyang University, Seoul 133-791*

[11]*University of Hawaii, Honolulu, Hawaii 96822*

[12]*High Energy Accelerator Research Organization (KEK), Tsukuba 305-0801*

[13]*Hiroshima Institute of Technology, Hiroshima 731-5193*

[14]*IKERBASQUE, Basque Foundation for Science, 48011 Bilbao*

[15]*Indian Institute of Technology Bhubaneswar, Satya Nagar 751007*

[16]*Indian Institute of Technology Guwahati, Assam 781039*

[17]*Indian Institute of Technology Madras, Chennai 600036*

[18]*Institute of High Energy Physics, Chinese Academy of Sciences, Beijing 100049*

[19]*Institute of High Energy Physics, Vienna 1050*

[20]*Institute for High Energy Physics, Protvino 142281*

[21]*INFN - Sezione di Torino, 10125 Torino*

[22]*Institute for Theoretical and Experimental Physics, Moscow 117218*

[23]*J. Stefan Institute, 1000 Ljubljana*

[24]*Kanagawa University, Yokohama 221-8686*

[25]*Institut für Experimentelle Kernphysik, Karlsruher Institut für Technologie, 76131 Karlsruhe*

[26]*Kavli Institute for the Physics and Mathematics of the Universe (WPI), University of Tokyo, Kashiwa 277-8583*

[27]*Department of Physics, Faculty of Sciences, King Abdulaziz University, Jeddah 21589*

[28]*Korea Institute of Science and Technology Information, Daejeon 305-806*

[29]*Korea University, Seoul 136-713*

[30]*Kyungpook National University, Daegu 702-701*

[31]*École Polytechnique Fédérale de Lausanne (EPFL), Lausanne 1015*

[32]*Faculty of Mathematics and Physics, University of Ljubljana, 1000 Ljubljana*
[33]*Luther College, Decorah, Iowa 52101*
[34]*University of Maribor, 2000 Maribor*
[35]*Max-Planck-Institut für Physik, 80805 München*
[36]*School of Physics, University of Melbourne, Victoria 3010*
[37]*Moscow Physical Engineering Institute, Moscow 115409*
[38]*Moscow Institute of Physics and Technology, Moscow Region 141700*
[39]*Graduate School of Science, Nagoya University, Nagoya 464-8602*
[40]*Kobayashi-Maskawa Institute, Nagoya University, Nagoya 464-8602*
[41]*Nara Women's University, Nara 630-8506*
[42]*National Central University, Chung-li 32054*
[43]*National United University, Miao Li 36003*
[44]*Department of Physics, National Taiwan University, Taipei 10617*
[45]*H. Niewodniczanski Institute of Nuclear Physics, Krakow 31-342*
[46]*Nippon Dental University, Niigata 951-8580*
[47]*Niigata University, Niigata 950-2181*
[48]*Osaka City University, Osaka 558-8585*
[49]*Pacific Northwest National Laboratory, Richland, Washington 99352*
[50]*Panjab University, Chandigarh 160014*
[51]*Peking University, Beijing 100871*
[52]*University of Pittsburgh, Pittsburgh, Pennsylvania 15260*
[53]*University of Science and Technology of China, Hefei 230026*
[54]*Seoul National University, Seoul 151-742*
[55]*Soongsil University, Seoul 156-743*
[56]*Sungkyunkwan University, Suwon 440-746*
[57]*School of Physics, University of Sydney, NSW 2006*
[58]*Department of Physics, Faculty of Science, University of Tabuk, Tabuk 71451*
[59]*Tata Institute of Fundamental Research, Mumbai 400005*
[60]*Excellence Cluster Universe, Technische Universität München, 85748 Garching*
[61]*Toho University, Funabashi 274-8510*
[62]*Tohoku Gakuin University, Tagajo 985-8537*
[63]*Tohoku University, Sendai 980-8578*
[64]*Tokyo Institute of Technology, Tokyo 152-8550*
[65]*Tokyo Metropolitan University, Tokyo 192-0397*
[66]*Tokyo University of Agriculture and Technology, Tokyo 184-8588*
[67]*CNP, Virginia Polytechnic Institute and State University, Blacksburg, Virginia 24061*
[68]*Wayne State University, Detroit, Michigan 48202*
[69]*Yamagata University, Yamagata 990-8560*
[70]*Yonsei University, Seoul 120-749*

The purely leptonic decay $B^+ \to \ell^+\nu_\ell$, where $\ell$ represents $e$, $\mu$ or $\tau$ [1], proceeds via annihilation of the $B^+$ meson's constituent quarks into a positively charged lepton and a neutrino of the same generation. In the Standard Model (SM), this annihilation is mediated by a $W^+$ boson. The branching fraction is calculated [1] by

$$\mathcal{B}(B^+ \to \ell^+\nu_\ell) = \frac{G_F^2 m_B m_\ell^2}{8\pi}\left(1 - \frac{m_\ell^2}{m_B^2}\right)^2 f_B^2 |V_{ub}|^2 \tau_B, \quad (1)$$

where $G_F$ is the Fermi coupling constant, $m_\ell$ is the mass of the charged lepton, $m_B$ is the mass of the $B^+$ meson, $\tau_B$ is the $B^+$ meson lifetime, $V_{ub}$ is an element of the Cabibbo-Kobayashi-Maskawa (CKM) matrix [2] governing the weak transition from the $b$ to the $u$ quark and $f_B$ is the $B$ decay constant. The estimated branching fractions using $|V_{ub}| = (3.51^{+0.15}_{-0.14}) \times 10^{-3}$ [3] from a fit to the full CKM unitarity triangle and $f_B = 186 \pm 4$ MeV [4] from lattice QCD calculations and the world average for all other parameters [3] are $\mathcal{B}(B^+ \to e^+\nu_e) = (7.9^{+0.8}_{-0.7}) \times 10^{-12}$, $\mathcal{B}(B^+ \to \mu^+\nu_\mu) = (3.4 \pm 0.3) \times 10^{-7}$, and $\mathcal{B}(B^+ \to \tau^+\nu_\tau) = (7.5 \pm 0.7) \times 10^{-5}$.

The $B^+ \to \tau^+\nu_\tau$ mode has been measured previously by the Belle [5] and BABAR [6] experiments, resulting in a combined branching fraction of $(1.05 \pm 0.25) \times 10^{-4}$ [3]. Due to the relatively small expected branching fractions, owing to helicity suppression in the SM, observation of the $B^+ \to e^+\nu_e$ and $B^+ \to \mu^+\nu_\mu$ decay modes remains a challenge. Currently, the most stringent upper limits of these decays are $\mathcal{B}(B^+ \to e^+\nu_e) < 9.8 \times 10^{-7}$ [7] and $\mathcal{B}(B^+ \to \mu^+\nu_\mu) < 1.0 \times 10^{-6}$ [8] at 90% confidence level (C.L.).

The $B^+ \to \ell^+\nu_\ell$ decays provide an excellent probe for new physics (NP), thanks to the small theoretical uncertainty in the SM branching fractions. For instance, in NP scenarios containing hypothetical particles such as the charged Higgs in 2-Higgs doublet models (type-II) [9] or the minimal supersymmetric model (MSSM) [10] or leptoquarks [11], the branching fractions of the $B^+ \to \ell^+\nu_\ell$ decays can be greatly enhanced.

Moreover, it has been suggested that the relative branching fractions of $B^+ \to \ell^+\nu_\ell$ to $B^+ \to \ell'^+\nu_{\ell'}$, $R^{\ell\ell'} = \mathcal{B}(B^+ \to \ell^+\nu_\ell)/\mathcal{B}(B^+ \to \ell'^+\nu_{\ell'})$ where $\ell \neq \ell'$, can be used to test the minimal flavor violation (MFV) hypothesis. In NP models with MFV [12], the ratios $R^{\ell\ell'}$ are expected to be nearly unmodified from SM expectations. However, in the framework of a grand unified theory (GUT) model, $B^+ \to \ell^+\nu_{\ell'}$ decays can additionally contribute as to increase the ratios $R^{e\mu}$ and $R^{e\tau}$ by more than 1 order of magnitude above SM expectations [13]. It has been also suggested that, in a general MSSM model at large $\tan\beta$ [14] with heavy squarks [15], the ratios $R^{e\tau}$ and $R^{\mu\tau}$ can deviate from SM expectations. Therefore measurements of $B^+ \to e^+\nu_e$ and $B^+ \to \mu^+\nu_\mu$ combined with the existing $B^+ \to \tau^+\nu_\tau$ determination can provide significant constraints on NP.

In this paper, we present a search for the previously unobserved $B^+ \to \ell^+\nu_\ell$ decays, using the hadronic tagging method, where $\ell$ stands for $e$ or $\mu$ [2]. In the hadronic tagging method, we fully reconstruct one of the $B$ mesons from the $\Upsilon(4S) \to B\bar{B}$ decay in a hadronic mode and then select the $B^+ \to \ell^+\nu_\ell$ signal from the rest of the event. The existing upper limits on the branching fraction determined using the hadronic tagging method are $\mathcal{B}(B^+ \to e^+\nu_e) < 5.2 \times 10^{-6}$ and $\mathcal{B}(B^+ \to \mu^+\nu_\mu) < 5.6 \times 10^{-6}$ [16] at 90%

[1] Charge-conjugate modes are implied throughout this paper unless stated otherwise.

[2] From this point and on, $\ell$ represents $e$ and $\mu$ only.

C.L. These are not as stringent as the limits mentioned above which were obtained by the so-called untagged method. But the hadronic tagging analysis is complementary to the untagged one in that it has a better sensitivity to discern new physics effects if it occurs.

By not explicitly reconstructing a $B$ meson, the untagged method does not fully utilize the information from the accompanying $B$ meson decay. While it leads to higher signal selection efficiencies, it suffers from a substantially higher background level. This could lead to ambiguities with other processes having similar decay signatures in case a signal is observed far in excess of the SM expectation. For instance, if an unknown heavy neutrino $\nu_h$ [17] appears in the $B^+ \to e^+\nu_h$ decay, it will be nearly impossible to distinguish it from the known process, $B^+ \to e^+\nu_e$, because of the limited kinematic precision of the untagged method.

In the hadronic tagging method, by fully reconstructing one $B$ meson ($B_{\rm tag}$), we have the best possible knowledge on the kinematics of the signal $B$ meson ($B_{\rm sig}$) in the event. This enables a precise measurement of the missing four-momentum of the neutrino in the $B^+ \to \ell^+\nu_\ell$ decays. As a result, the momentum of the charged lepton in the $B^+ \to \ell^+\nu_\ell$ signal can be determined with an order-of-magnitude higher resolution compared to the untagged method [7]. This results in a very strong background suppression and provides an extra constraint for identifying the nature of the undetected particle.

The data sample used in this analysis was collected with the Belle detector [18] at the KEKB asymmetric-energy $e^+e^-$ collider [19]. The sample corresponds to an integrated luminosity of 711 fb$^{-1}$ or $772 \times 10^6$ $B\bar{B}$ pairs, collected on the $\Upsilon(4S)$ resonance at a center-of-mass (CM) energy ($\sqrt{s}$) of 10.58 GeV.

The Belle detector is a large-solid-angle spectrometer that consists of a silicon vertex detector (SVD), a 50-layer central drift chamber (CDC), aerogel threshold Cherenkov counters (ACC), an array of a barrel-like arrangement of time-of-flight scintillation counters (TOF), and an electromagnetic calorimeter comprised of 8736 CsI(Tl) crystals (ECL) located inside a superconducting solenoid coil that provides a 1.5 T magnetic field. An iron flux return located outside of the coil is instrumented to detect $K_L^0$ mesons and to identify muons (KLM).

Electron identification is based on the ratio between the cluster energy in the ECL and the track momentum from the CDC ($E/p$), the specific ionization $dE/dx$ in the CDC, the position and shower shape of the cluster in the ECL and the response from the ACC. Muon identification is based on the hit position and the penetration depth in the KLM. In the momentum range of interest in this analysis, the electron (muon) identification efficiency is above 90% and the hadron fake rate is under 0.5% (5%). A more detailed description can be found elsewhere [20].

The $B_{\rm tag}$ candidates are reconstructed in 615 exclusive charged $B$ meson decay channels with a reconstruction algorithm based on a hierarchical neural network [21]. To compensate for the difference between the MC and data in the $B_{\rm tag}$ tagging efficiency ($\epsilon_{\rm tag}$) due to uncertainties in branching fractions and dynamics of hadronic modes, we apply a correction obtained from a control sample study [22] in which the signal-side $B$ meson decays via five semileptonic $B^+$ decay modes: $B^+ \to \bar{D}^0(K^+\pi^-)\ell^+\nu_\ell$, $B^+ \to \bar{D}^0(K^+\pi^-\pi^0)\ell^+\nu_\ell$, $B^+ \to \bar{D}^0(K^+\pi^-\pi^-\pi^+)\ell^+\nu_\ell$, $B^+ \to \bar{D}^{*0}[\bar{D}^0(K^+\pi^-)\pi^0]\ell^+\nu_\ell$, and $\bar{D}^{*0}[\bar{D}^0(K^+\pi^-)\gamma]\ell^+\nu_\ell$. The MC efficiency is corrected according to the $B_{\rm tag}$ decay mode as well as the output of the hadronic tagging algorithm ($o_{\rm tag}$) on an event-by-event basis. The $o_{\rm tag}$ distribution peaks near zero for combinatorial or continuum backgrounds, and near one for well

reconstructed $B_{\rm tag}$ candidates.

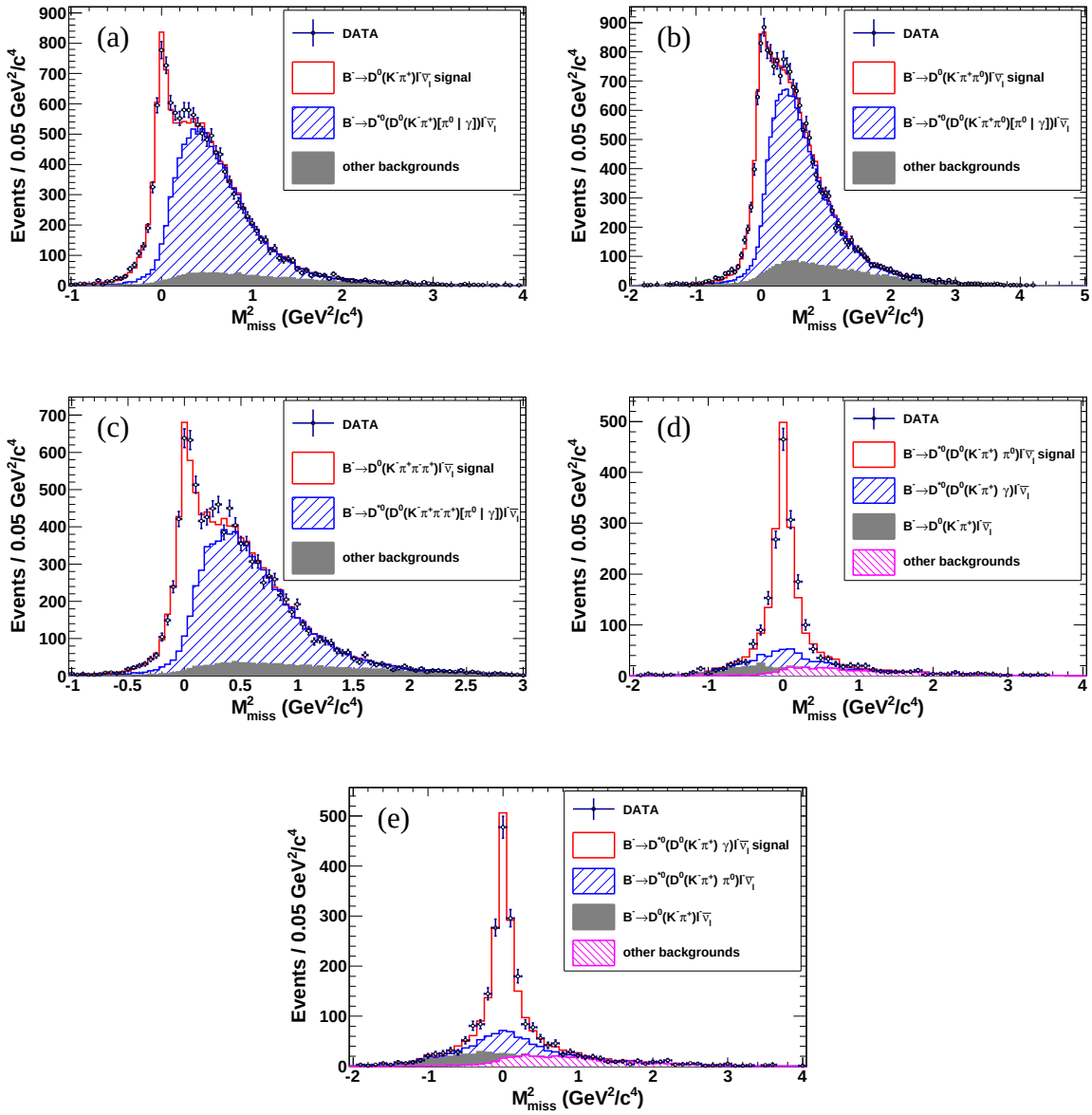


FIG. 1: Fits to the $M^2_{\rm miss}$ distribution in data using the tagging efficiency corrected MC histogram templates in each of the (a) $B^+ \to \bar{D}^0(K^+\pi^-)\ell^+\nu_\ell$, (b) $B^+ \to \bar{D}^0(K^+\pi^-\pi^0)\ell^+\nu_\ell$, (c) $B^+ \to \bar{D}^0(K^+\pi^-\pi^-\pi^+)\ell^+\nu_\ell$, (d) $B^+ \to \bar{D}^{*0}(\bar{D}^0[K^+\pi^-]\pi^0)\ell^+\nu_\ell$, and (e) $B^+ \to \bar{D}^{*0}(\bar{D}^0[K^+\pi^-]\gamma)\ell^+\nu_\ell$ control sample modes. The other backgrounds component as listed in the legends is consisted of $b \to c$ decays, $e^+e^- \to q\bar{q}$ ($q = u, d, s, c$) decays, and $b \to u\ell^-\bar{\nu}_\ell$ decays.

The correction factor for each $B_{\rm tag}$ decay mode is determined by the comparison of the number of events in MC and data from a one-dimensional binned maximum likelihood (ML) fit using histogram templates [23], which take account of both the data and MC statistical uncertainty, to the distribution of the square of the missing particle's unde-

tected four-momentum ($M^2_{\rm miss}$). Here $M^2_{\rm miss}$ is expected to peak near zero for correctly reconstructed $B^+ \to \bar{D}^{(*)0}\ell^+\nu_\ell$ events in which the only missing particle is a massless neutrino as displayed in Figure 1. The correction factor is then obtained from each of the five control samples and we apply the averaged factor in our analysis. The systematic uncertainty of the $\epsilon_{\rm tag}$ correction is estimated including the statistical precision of the correction, the uncertainty of the branching fraction of the control sample modes [3], the effects of background-modeling to the $M^2_{\rm miss}$ fitting, and the uncertainty due to the particle identification used in reconstructing the $D^{*0}$ mesons obtained by studying the $D^{*+} \to D^0\pi^+$ decay followed by the $D^0 \to K^-\pi^+$ decay. Including the systematic uncertainty, we finally obtain the correction factor as $0.71 \pm 0.05$ in both the $B^+ \to e^+\nu_e$ and $B^+ \to \mu^+\nu_\mu$ signal MC samples, with a total fractional uncertainty of 6.4% to the correction factor.

In 42% of the events for both the $B^+ \to e^+\nu_e$ and $B^+ \to \mu^+\nu_\mu$ signal MC samples, we find multiple $B_{\rm tag}$ candidates. In such cases, we select the $B_{\rm tag}$ candidate with the highest $o_{\rm tag}$. To ensure a well reconstructed $B_{\rm tag}$ candidate, we further require $o_{\rm tag}$, the energy difference, $\Delta E = E^*_{B_{\rm tag}} - \sqrt{s}/2$, and the beam-constrained-mass $M_{\rm bc} = \sqrt{s/4 - |\vec{p}^{\,*}_{B_{\rm tag}}|^2}$, to satisfy $o_{\rm tag} > 0.0025$, $|\Delta E| < 0.05$ GeV, and $5.27\ {\rm GeV}/c^2 < M_{\rm bc} < 5.29\ {\rm GeV}/c^2$, where $E^*_{B_{\rm tag}}$ and $\vec{p}^{\,*}_{B_{\rm tag}}$ are the $B_{\rm tag}$ energy and momentum, respectively, in the CM frame. The efficiencies of this $B_{\rm tag}$ reconstruction procedure on events containing signal decays are: $\epsilon_{\rm tag} = 0.29 \pm 0.02$ % for the $B^+ \to e^+\nu_e$ and $\epsilon_{\rm tag} = 0.30 \pm 0.02$ % for the $B^+ \to \mu^+\nu_\mu$. These $\epsilon_{\rm tag}$ values include the correction factor described above.

On the $B_{\rm sig}$ side, we require exactly one remaining track in the detector and that it be identified as an electron or a muon. Since the signal mode is a two-body decay of a $B^+$ meson, the lepton momentum in the rest frame of the $B_{\rm sig}$ ($p^B_\ell$) peaks sharply around 2.64 GeV/$c$. To utilize this feature while keeping a sideband available for background estimation, the lepton candidates are initially required to have a momentum above 1.8 GeV/$c$ in the laboratory frame. They are also required to satisfy $|dz| < 1.5$ cm and $dr < 0.05$ cm, where $dz$ and $dr$ are impact parameters of the track along the beam direction and in the perpendicular plane, respectively.

To suppress the continuum background ($e^+e^- \to q\bar{q}$ [$q = u, d, s, c$]), we use the event shape difference between $B\bar{B}$ events and continuum. Since each $\Upsilon(4S)$ decays nearly at rest, the decay products of the resulting $B\bar{B}$ pair have a spherical event shape. On the other hand, continuum event shapes tend to be two-jet-like. We define $\theta_{\rm T}$ as the angle between the momentum of the signal lepton and the unit vector $\hat{n}$ that maximizes $\Sigma_i|\hat{n}\cdot\vec{p}_i|/|\vec{p}_i|$, where the index $i$ runs over all particles used for $B_{\rm tag}$ reconstruction. We require $\cos\theta_{\rm T} < 0.9$ and $\cos\theta_{\rm T} < 0.8$ for $B^+ \to e^+\nu_e$ and $B^+ \to \mu^+\nu_\mu$, respectively. In the muon mode, we expect a larger continuum background compared to the electron mode due to the higher hadron misidentification rate. Therefore, we apply a more stringent $\cos\theta_{\rm T}$ criterion for this mode.

For signal events, we expect no detectable particles left after removing the signal lepton and the particles associated with the $B_{\rm tag}$. Therefore, there should be no extra energy deposits in the ECL except for the small contributions from split-off showers and beam background. We define the extra energy ($E_{\rm ECL}$) as the sum of the energy from the neutral clusters not associated with $B_{\rm tag}$ or the signal lepton deposited in the ECL. In the $E_{\rm ECL}$ calculation, minimum thresholds of 50 MeV for the barrel ($32.2^\circ < \theta < 128.7^\circ$), 100 MeV for the forward end-cap ($12.4^\circ < \theta < 31.4^\circ$), and 150 MeV for the backward end-cap

($130.7^\circ < \theta < 155.1^\circ$) of the calorimeter are required, where $\theta$ is the cluster's polar angle relative to the beam direction [18]. Higher thresholds are applied for the end-cap regions due to the severity of beam background there. We require $E_{\rm ECL} < 0.5$ GeV for both $B^+ \to e^+\nu_e$ and $B^+ \to \mu^+\nu_\mu$.

We identify signal events with $p_\ell^B$. By studying the signal MC samples, we demand that each signal event satisfies 2.6 GeV/$c$ $< p_\ell^B <$ 2.7 GeV/$c$ for both $B^+ \to e^+\nu_e$ and $B^+ \to \mu^+\nu_\mu$.

Dominant backgrounds arise from decays with neutral particles not detected or used in the reconstruction of the $B_{\rm tag}$ and a high momentum track that falls in the $p_\ell^B$ signal region. For the $B^+ \to e^+\nu_e$, $B^+ \to \pi^+K^0$, $B^+ \to \ell^+\nu_\ell\gamma$, and $B^+ \to \pi^0\ell^+\nu_\ell$ decays in our sample constitute 100% of the background events in the $p_\ell^B$ signal region. For the $B^+ \to \mu^+\nu_\mu$, $B^+ \to \pi^+K^0$, $B^+ \to K^+\pi^0$, $B^+ \to \ell^+\nu_\ell\gamma$, and $B^+ \to \pi^0\ell^+\nu_\ell$ decays constitute 84.7% of the background events in the $p_\ell^B$ signal region with the remainder coming from all other $b \to u\ell^-\bar{\nu}_\ell$ decays. For an accurate modeling of the background probability density function (PDF) near the $p_\ell^B$ signal region, we generate dedicated MC samples for $B^+ \to \pi^+K^0$, $B^+ \to K^+\pi^0$, $B^+ \to \ell^+\nu_\ell\gamma$, and $B^+ \to \pi^0\ell^+\nu_\ell$ decays. For the $B^+ \to \ell^+\nu_\ell\gamma$ process, which has not been observed yet, we assume a branching fraction of $\mathcal{B}(B^+ \to \ell^+\nu_\ell\gamma) = 5 \times 10^{-6}$ [24].

We define the sideband of the $p_\ell^B$ as 2.0 GeV/$c$ $< p_\ell^B <$ 2.5 GeV/$c$. The $p_\ell^B$ sideband is dominated by the $b \to c$ and $b \to u\ell^-\bar{\nu}_\ell$ decays. Out of all background events in the $p_\ell^B$ sideband, each $b \to c$ and $b \to u\ell^-\bar{\nu}_\ell$ decay contributes 55% (60%) and 39% (34%) for the $B^+ \to e^+\nu_e$ ($B^+ \to \mu^+\nu_\mu$). The remaining 6% of the background in the $p_\ell^B$ sideband originates from the $B^+ \to \ell^+\nu_\ell\gamma$ decay and the $b \to s, d$ processes aside from $B^+ \to \pi^+K^0$ or $B^+ \to K^+\pi^0$ for both searches. $B^+ \to \bar{D}^{*0}\ell^+\nu_\ell$ and $B^+ \to \bar{D}^0\ell^+\nu_\ell$ decays are found to be composing the $b \to c$ decays for the $B^+ \to e^+\nu_e$ ($B^+ \to \mu^+\nu_\mu$) at rates of 67% (64%) and 24% (21%), respectively, and are treated separately from the other $b \to c$ decays.

Continuum events are found to be negligible in both the $p_\ell^B$ sideband and $p_\ell^B$ signal regions.

We calculate the branching fraction as

$$\mathcal{B}(B^+ \to \ell^+\nu) = \frac{N_{\rm obs} - N_{\rm exp}^{\rm bkg}}{2 \cdot \epsilon_{\rm s} \cdot N_{B^+B^-}}, \tag{2}$$

where $N_{\rm obs}$ is the observed yield of the data sample in the $p_\ell^B$ signal region, $N_{\rm exp}^{\rm bkg}$ is the expected number of background events in the $p_\ell^B$ signal region, $\epsilon_{\rm s}$ is the total signal selection efficiency, and $N_{B^+B^-}$ is the number of $\Upsilon(4S) \to B^+B^-$ events in the data sample. Using $\mathcal{B}(\Upsilon(4S) \to B^+B^-) = 0.513 \pm 0.006$ [3], we estimate $N_{B^+B^-}$ as $(396 \pm 7) \times 10^6$.

We obtain $N_{\rm exp}^{\rm bkg}$ by fitting the $p_\ell^B$ sideband of the data sample, with a PDF obtained from the background MC. We then estimate the expected background yield in the $p_\ell^B$ signal region from the ratio of the fitted background MC yields in the $p_\ell^B$ sideband and the $p_\ell^B$ signal region.

The systematic uncertainties on $N_{\rm exp}^{\rm bkg}$ are estimated according to the uncertainties in the background PDF parameters, the branching fraction of background decays, and the statistics of the data sample in the $p_\ell^B$ sideband. We vary each source in turn by its uncertainty ($\pm 1\sigma$) and the resulting deviations in $N_{\rm exp}^{\rm bkg}$ are added in quadrature. To calculate the effect of the branching fraction uncertainties of the background modes, we

refer to the experimental measurements [3] for the $B^+ \to \bar{D}^{(*)0}\ell^+\nu_\ell$, $B^+ \to \pi^0\ell^+\nu_\ell$, $B^+ \to \pi^+K^0$, and $B^+ \to K^+\pi^0$ modes, and vary each branching fraction one by one from the world-average value by its error. For the $B^+ \to \ell^+\nu_\ell\gamma$, an uncertainty of $\pm 50\%$ is applied. For modes where a clear estimate of the background level is not available, we assume a conservative branching fraction uncertainty of $^{+100}_{-50}\%$. The values of $N^{\rm bkg}_{\rm exp}$ and their uncertainties for both $B^+ \to e^+\nu_e$ and $B^+ \to \mu^+\nu_\mu$ decays are listed in Table I.

TABLE I: Summary of the signal selection efficiency ($\epsilon_{\rm s}$), the number of events observed in the $p^B_\ell$ signal region ($N_{\rm obs}$), and the expected background yield in the $p^B_\ell$ signal region ($N^{\rm bkg}_{\rm exp}$) for the $B^+ \to \ell^+\nu_\ell$ search.

| Mode | $\epsilon_{\rm s}$ [%] | $N_{\rm obs}$ | $N^{\rm bkg}_{\rm exp}$ |
|---|---|---|---|
| $B^+ \to e^+\nu_e$ | $0.086 \pm 0.007$ | 0 | $0.10 \pm 0.04$ |
| $B^+ \to \mu^+\nu_\mu$ | $0.102 \pm 0.008$ | 0 | $0.26^{+0.09}_{-0.08}$ |

TABLE II: Summary of multiplicative systematic uncertainties related to the $\epsilon_{\rm s}N_{B^+B^-}$ calculation, in percent.

| Source | $B^+ \to e^+\nu_e$ | $B^+ \to \mu^+\nu_\mu$ |
|---|---|---|
| $N_{B^+B^-}$ | 1.8 | 1.8 |
| Lepton ID | 2.0 | 2.3 |
| MC statistics | 1.4 | 1.3 |
| Tracking efficiency | 0.35 | 0.35 |
| $\epsilon_{\rm tag}$ correction | 6.4 | 6.4 |
| $p^B_\ell$ Shape | 3.6 | 3.6 |
| Total | 8.0 | 8.0 |

The efficiencies $\epsilon_{\rm s}$ are $0.086 \pm 0.007$ and $0.102 \pm 0.008$ for $B^+ \to e^+\nu_e$ and $B^+ \to \mu^+\nu_\mu$, respectively, as summarized in Table I. The uncertainties of $\epsilon_{\rm s}$ are calculated from the following sources: lepton identification, signal MC statistical error, track finding uncertainties of the signal lepton, $\epsilon_{\rm tag}$ correction, and $p^B_\ell$ shape.

The lepton identification efficiency correction is estimated by comparing the efficiency difference between the data and MC using $\gamma\gamma \to e^+e^-/\mu^+\mu^-$ processes, from which we obtain a 2.0% uncertainty for $B^+ \to e^+\nu_e$ and 2.3% for $B^+ \to \mu^+\nu_\mu$. The uncertainty due to signal MC statistics is 1.4% for $B^+ \to e^+\nu_e$ and 1.3% for $B^+ \to \mu^+\nu_\mu$. The track-finding uncertainty is obtained by studying the partially reconstructed $D^{*+} \to D^0\pi^+$, $D^0 \to K^0_S\pi^+\pi^-$, and $K_S \to \pi^+\pi^-$ decay chain, where one of the $K^0_S$ daughters is not explicitly reconstructed. We compare, between data and MC, the efficiency of finding the $K^0_S$ daughter pion which is not explicitly used in the partial $D^*$ reconstruction and estimate a contribution of 0.35% uncertainty for both $B^+ \to e^+\nu_e$ and $B^+ \to \mu^+\nu_\mu$ modes. We also include the 6.4% $\epsilon_{\rm tag}$ correction uncertainty mentioned earlier.

To account for the difference of $p^B_\ell$ shapes in the signal MC and the data, we study $B^+ \to \bar{D}^0\pi^+$ decays as a control sample. The control sample is similar to our signal

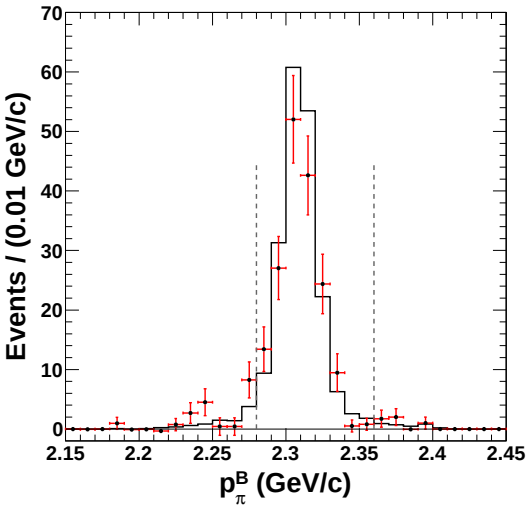


FIG. 2: The $p_\pi^B$ distributions of the $B^+ \to \bar{D}^0\pi^+$ control sample study. The points with error bars indicate the background-subtracted data and the solid histogram shows the MC distribution. The region between the two dashed lines represents the $p_\pi^B$ selection region for the control sample study.

decay since it is also a two-body decay of a $B^+$ meson. The $\bar{D}^0$ meson is identified in the $\bar{D}^0 \to K^+\pi^-$ and $\bar{D}^0 \to K^+\pi^-\pi^+\pi^-$ decay channels. We follow the same analysis procedure as in the $B^+ \to \ell^+\nu_\ell$ analysis, where the $\pi^+$ from the primary decay of the $B^+$ meson (primary $\pi^+$), is treated as the lepton and the $\bar{D}^0$ decay products as a whole are treated as the invisible neutrino. We compare the distributions of the primary $\pi^+$ momentum in the rest frame of the signal $B$ ($p_\pi^B$) between the background subtracted data sample and the control sample MC, which are displayed in Fig. 2.

We estimate the $p_\ell^B$ shape correction factor as the ratio of the $p_\pi^B$ selection efficiencies between the background-subtracted data and MC for the control mode. The yields are compared for the wide (2.15 GeV/$c$ < $p_\pi^B$ < 2.45 GeV/$c$) and the peak (2.28 GeV/$c$ < $p_\pi^B$ < 2.36 GeV/$c$) region, separately for data and MC. By comparing the ratios of the peak region yield to that of the wide region, we obtain the $p_\ell^B$ shape correction factor as $0.953 \pm 0.034$, where the error includes both the statistical uncertainty of the study as well as systematic uncertainties in fitting. With this correction applied to the MC sample, the control sample yield of data and MC agree within $0.3\sigma$.

The total systematic uncertainty related to $\epsilon_{\rm s} N_{B^+B^-}$ is 8.0% for both $B^+ \to e^+\nu_e$ and $B^+ \to \mu^+\nu_\mu$. The multiplicative uncertainties related to $\epsilon_{\rm s} N_{B^+B^-}$ are summarized in Table II.

In the $p_\ell^B$ signal region, we observe no events for either search as shown in Fig. 3. We set 90% C.L. branching fraction upper limits using the POLE program [25] based on a frequentist approach [26]. In the calculation, we assume a Gaussian distribution of $N_{\rm exp}^{\rm bkg}$, with a conservative assumption by choosing the larger deviation of the asymmetric uncertainty in $N_{\rm exp}^{\rm bkg}$. We obtain upper limits of the branching fraction for each mode as $\mathcal{B}(B^+ \to e^+\nu_e) < 3.5 \times 10^{-6}$ and $\mathcal{B}(B^+ \to \mu^+\nu_\mu) < 2.7 \times 10^{-6}$ at 90% C.L, which include the systematic uncertainties.

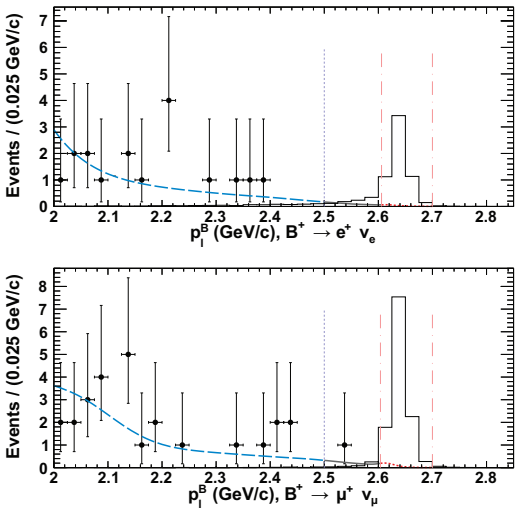


FIG. 3: The $p_\ell^B$ distributions for $B^+ \to e^+\nu_e$ (top) and $B^+ \to \mu^+\nu_\mu$ (bottom). The points with error bars are the experimental data. The solid histograms are for the signal MC distributions which are scaled up by a factor of $10^6$ (40) from the SM expectation for $B^+ \to e^+\nu_e$ ($B^+ \to \mu^+\nu_\mu$). The dashed (blue) curves show the background PDF fitted in the sideband region (2.0 GeV/$c < p_\ell^B <$ 2.5 GeV/$c$). The vertical dotted line shows the upper bound of the $p_\ell^B$ sideband, while the region between the two dot-dashed (red) vertical lines correspond to the $p_\ell^B$ signal region.

In summary, we have searched for the leptonic decays $B^+ \to e^+\nu_e$ and $B^+ \to \mu^+\nu_\mu$ with the hadronic tagging method using a data sample containing $772 \times 10^6$ $B\bar{B}$ events collected by the Belle experiment. We find no evidence of $B^+ \to e^+\nu_e$ and $B^+ \to \mu^+\nu_\mu$ processes. We set the upper limits of the branching fraction at $\mathcal{B}(B^+ \to e^+\nu_e) < 3.5\times10^{-6}$ and $\mathcal{B}(B^+ \to \mu^+\nu_\mu) < 2.7 \times 10^{-6}$ at 90% C.L, which are by far the most stringent limits obtained with the hadronic tagging method. Given the low background level demonstrated in this search, we expect more stringent constraints on the new physics models to be set by Belle II [27], the next generation $B$ factory experiment.

We thank the KEKB group for the excellent operation of the accelerator; the KEK cryogenics group for the efficient operation of the solenoid; and the KEK computer group, the National Institute of Informatics, and the PNNL/EMSL computing group for valuable computing and SINET4 network support. We acknowledge support from the Ministry of Education, Culture, Sports, Science, and Technology (MEXT) of Japan, the Japan Society for the Promotion of Science (JSPS), and the Tau-Lepton Physics Research Center of Nagoya University; the Australian Research Council and the Australian Department of Industry, Innovation, Science and Research; Austrian Science Fund under Grant No. P 22742-N16; the National Natural Science Foundation of China under Contracts No. 10575109, No. 10775142, No. 10825524, No. 10875115, No. 10935008 and No. 11175187; the Ministry of Education, Youth and Sports of the Czech Republic under Contract No. LG14034; the Carl Zeiss Foundation, the Deutsche Forschungsgemeinschaft and the VolkswagenStiftung; the Department of Science and Technology of India; the Istituto Nazionale di Fisica Nucleare of Italy; the WCU program of the Ministry of Education Science and Technology, National Research Foundation of Korea Grants

No. 2011-0029457, No. 2012-0008143, No. 2012R1A1A2008330, No. 2013R1A1A3007772; the BRL program under NRF Grant No. KRF-2011-0020333, No. KRF-2011-0021196, Center for Korean J-PARC Users, No. NRF-2013K1A3A7A06056592; the BK21 Plus program and the GSDC of the Korea Institute of Science and Technology Information; the Polish Ministry of Science and Higher Education and the National Science Center; the Ministry of Education and Science of the Russian Federation and the Russian Federal Agency for Atomic Energy; the Slovenian Research Agency; the Basque Foundation for Science (IKERBASQUE) and the UPV/EHU under program UFI 11/55; the Swiss National Science Foundation; the National Science Council and the Ministry of Education of Taiwan; and the U.S. Department of Energy and the National Science Foundation. This work is supported by a Grant-in-Aid from MEXT for Science Research in a Priority Area ("New Development of Flavor Physics") and from JSPS for Creative Scientific Research ("Evolution of Tau-lepton Physics").

[1] D. Silverman and H. Yao, Phys. Rev. D **38**, 214 (1988).
[2] N. Cabibbo, Phys. Rev. Lett **10**, 531 (1963); M. Kobayashi and T. Maskawa, Prog. Theor. Phys. **49**, 652 (1973).
[3] J. Beringer *et al.* (Particle Data Group), Phys. Rev. D **86**, 010001 (2012) and 2013 partial update for the 2014 edition.
[4] R. J. Dowdall *et al.* (HPQCD Collaboration), Phys. Rev. Lett. **110**, 222003 (2013).
[5] K. Hara *et al.* (Belle Collaboration), Phys. Rev. D **82**, 071101(R) (2010); K. Hara *et al.* (Belle Collaboration), Phys. Rev. Lett. **110**, 131801 (2013).
[6] B. Aubert *et al.* (BABAR Collaboration) Phys. Rev. D **76**, 052002 (2007); B. Aubert *et al.* (BABAR Collaboration), Phys. Rev. D **77**, 011107(R) (2008).
[7] N. Satoyama *et al.* (Belle Collaboration), Phys. Lett. B **647**, 67 (2007).
[8] B. Aubert *et al.* (BABAR Collaboration), Phys. Rev. D **79**, 091101 (2009).
[9] W.-S. Hou, Phys. Rev. D **48**, 2342 (1993).
[10] S. Baek and Y. G. Kim, Phys. Rev. D **60**, 077701 (1999).
[11] H. Georgi and S. L. Glashow, Phys. Rev. Lett. **32**, 438 (1974).
[12] V. Cirigliano, B. Grinstein, G. Isidori, and M. B. Wise, Nucl. Phys. **B728**, 121 (2005).
[13] A. Filipuzzi and G. Isidori, Eur. Phys. J. C **64**, 55 (2009).
[14] The parameter $\tan\beta$ is the ratio of the vacuum expectation values of the two Higgs fields; see A. Djouadi and J. Quevillon, J. High Energy Phys. 10 (2013) 028.
[15] G. Isidori and P. Paradisi, Phys. Lett. B **639**, 499 (2006).
[16] B. Aubert *et al.* (BABAR Collaboration), Phys. Rev. D **77**, 091104 (2008).
[17] T. Asaka, S. Blanchet, and M. Shaposhnikov, Phys. Lett. B **631**, 151 (2005); T. Asaka and M. Shaposhnikov, Phys. Lett. B **620**, 17 (2005).
[18] A. Abashian *et al.* (Belle Collaboration), Nucl. Instrum. Methods Phys. Res. Sect. A **479**, 117 (2002); also see detector section in J.Brodzicka *et al.*, Prog. Theor. Exp. Phys. (2012) 04D001.
[19] S. Kurokawa and E. Kikutani, Nucl. Instrum. Methods Phys. Res. Sect. A **499**, 1 (2003), and other papers included in this volume; T.Abe *et al.*, Prog. Theor. Exp. Phys. (2013) 03A001 and following articles up to 03A011.

[20] K. Hanagaki *et al.*, Nucl. Instrum. Methods Phys. Res., Sect. A **485**, 490 (2002); A. Abashian *et al.*, Nucl. Instrum. Methods Phys. Res., Sect. A **491**, 69 (2002).
[21] M. Feindt *et al.*, Nucl. Instrum. Methods Phys. Res., Sect. A **654**, 432 (2011).
[22] A. Sibidanov *et al.* (Belle Collaboration), Phys. Rev. D **88**, 032005 (2013).
[23] R. Barlow and C. Beeston, Comput. Phys. Comm. **77** (1993) 219-228.
[24] G. Korchemsky, D. Pirjol and T.-M. Yan, Phys. Rev. D **61**, 114510 (2000).
[25] J. Conrad *et al.*, Phys. Rev. D **67**, 012002 (2003).
[26] G. J. Feldman and R. D. Cousins, Phys. Rev. D **57**, 3873 (1998).
[27] T. Abe *et al.* (Belle Collaboration), arXiv:1011.0352v1 [physics.ins-det] (2010).